



## Communication

# A Compact Dual-Band Quasi-Elliptic Filter Employing Meander-Line- and CRLH-Based SIW Triplets

Yilong Zhu<sup>1,2</sup>, Yuandan Dong<sup>1</sup>, Lin Gu<sup>1</sup>, Deisy Formiga Mamedes<sup>3</sup>, and Jens Bornemann<sup>3</sup>

1. School of Electronic Science and Engineering, University of Electronic Science and Technology of China, Chengdu 611731, China

2. Aerospace Information Research Institute, Chinese Academy of Sciences, Beijing 100094, China

3. Department of Electrical and Computer Engineering, University of Victoria, Victoria, BC V8W 2Y2, Canada

Corresponding author: Yuandan Dong, Email: [ydong@uestc.edu.cn](mailto:ydong@uestc.edu.cn).

Copyright © 2024 The Author(s). This is a gold open access article under a Creative Commons Attribution License (CC BY 4.0).

**Abstract** — A compact dual-band quasi-elliptic filter with high selectivity is developed and investigated in this communication. It employs two hybrid-structure substrate integrated waveguide (SIW) triplets, which show completely inverse transfer responses under the same conditions of inductive cross coupling. The first meander-line-based triplet is able to produce a transmission zero (TZ) above the passband. Whereas the second SIW triplet, which is composed by a composite right/left-handed (CRLH) resonator, creates a TZ below the passband. By utilizing these features, a dual-band quasi-elliptic filter based on SIW dual-mode resonances ( $TE_{101}$  and  $TE_{201}$ ), whose operating frequencies are allocated at 8 GHz and 10 GHz, is designed for demonstration. The design process, principles, and experiments are carefully described in this communication. The measured and simulated results are in good agreement, indicating excellent electrical performance with low loss, compact device size and high selectivity. The most notable point is that a dual-band quasi-elliptic filter on SIW platforms is obtained with all inductive couplings for the first time, which shows a unique benefit in eliminating negative-coupling structures while permitting miniaturization for SIW dual-band filter design.

**Keywords** — Dual-band quasi-elliptic filter, High selectivity, Compact size, Meander-line and CRLH resonators, Substrate integrated waveguide.

**Citation** — Yilong Zhu, Yuandan Dong, Lin Gu, *et al.*, “A compact dual-band quasi-elliptic filter employing meander-line- and CRLH-based SIW triplets,” *Electromagnetic Science*, vol. 2, no. 2, article no. , 2024. doi: [10.23919/emsci.2024.0017](https://doi.org/10.23919/emsci.2024.0017).

## I. Introduction

To access multiple services and channels with a single multimode terminal, dual-band filters have drawn tremendous attention for communication systems. The typical method of implementing dual-band responses is to use parallel independent single-band filters [1]–[7]. Utilizing dual-mode resonances [8]–[12] has recently become another popular design technique for dual-band filters, especially for those on substrate integrated waveguide (SIW) platforms [13]–[19], which can be operated at high frequency with fair quality factors. For example, by using dual-mode resonances of the  $TE_{101}$  and  $TE_{201}$  (or  $TE_{102}/TE_{301}$ ) modes, dual-band SIW filters were obtained in [13]–[16]. However, their selectivity suffers because of a lack of transmission zeros (TZs). To achieve highly selective dual-band filters, negative-coupling

structures, such as S-shaped slots [17], [18], interdigital-like formats [19], and grounded coplanar waveguide (GCPW) lines [20], are generally required to create TZs on both sides of passbands. However, this increases structural complexity and introduces some radiation loss. To eliminate negative-coupling structures, it has been proposed to etch microstrip resonators with electric mutual couplings between the SIW cavities [21]. This transforms the cross coupling from electric to magnetic, thereby permitting the use of simple SIW inductive coupling windows.

Another technique for eliminating negative-coupling structures was proposed in our previous publication [22]; it utilizes two types of SIW triplets loaded by meander-line resonators and composite right/left-handed (CRLH), as presented in Figures 1(a) and (b), respectively. Two single-band quasi-elliptic filters with all inductive couplings are

then originally achieved through series and parallel combinations of these two SIW triplets.

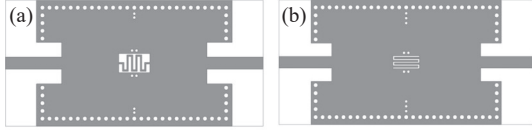


**Figure 1** (a) Meander-line-based and (b) CRLH-based SIW triplets.

The purpose of this communication is to spearhead such applications for the design of SIW dual-band filters with quasi-elliptic responses. First, SIW dual-mode resonances, namely, the  $TE_{101}$  and  $TE_{201}$  modes, are used to create the two passbands. To develop different triplets for these two SIW modes, the procedures of setting up the meander-line and CRLH resonators are illustrated sequentially, including the numbers and arrangements of these resonators. A prototype filter, whose center frequencies are allocated at 8 GHz and 10 GHz, is implemented for validation. The measured results indicate that the proposed filter has the advantages of low loss, compact size and high selectivity with a TZ created at both sides of each passband. This technique is highly valuable to engineers in applications of dual-band quasi-elliptic filters with all inductive couplings.

## II. Meander-Line- and CRLH-Based SIW Triplets

Although the two novel SIW triplets were investigated in our previous publication [22], we would like to provide a very brief introduction to them for the convenience of the reader. As presented in Figures 1(a) and (b), these SIW triplets are constructed by etching a meander-line resonator and a CRLH resonator in their centers, respectively. Two pairs of metallic via arrays are placed around the two microstrip resonators to adjust the couplings between them and the SIW cavities. Note that an inductive cross coupling is introduced by symmetric coupling windows constructed between the SIW cavities.

The coupling topologies of these two SIW triplets are depicted in Figure 2. The SIW cavities and the meander-line resonator are considered traditional resonant nodes, whose phase shifts are  $+90^\circ$  below and  $-90^\circ$  above their resonances, whereas the CRLH resonator shows completely inverse phase shifts of  $-90^\circ$  and  $+90^\circ$  around its resonance. Notably, all the couplings are inductive between any two resonant nodes in the two topologies.

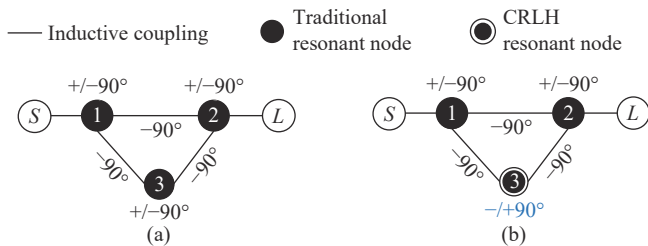


**Figure 2** (a) Coupling topology of the meander-line-based SIW triplet. (b) Coupling topology of the CRLH-based SIW triplet.

To investigate the transfer features of the SIW triplets, they are represented by their equivalent network circuits in Figure 3. For the meander-line SIW triplet, all resonators can be considered as shunt LC resonant pairs. For the CRLH-SIW triplet, however, the CRLH resonator is equivalent to a  $\pi$ -type LC resonant circuit because of the dominant series capacitance among the electrodes. To maintain the same input admittance and resonant frequency as the shunt LC pairs, the series capacitance herein is set as a frequency-dependent parameter, as shown in Figure 3(b). For both circuits, the couplings between any two resonators are inductive, which can be realized by  $J$  inverters with a phase shift of  $-90^\circ$ .

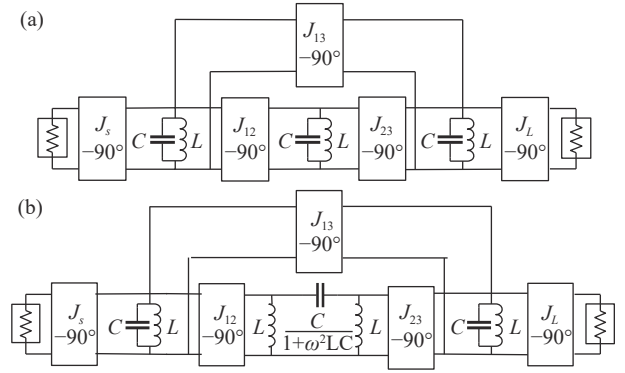


**Figure 3** (a) Network circuit of the meander-line-formed SIW triplet; (b) Network circuit of the CRLH-formed SIW triplet.

The  $S_{21}$  parameters can be obtained by extracting the odd and even components of the circuits in Figure 3. If we let  $S_{21}$  equal zero, the positions of the TZs can be calculated through the derivatives shown in (1) and (2):

$$\frac{\omega_{z1}^2 LC - 1}{\omega_{z1} L} = \frac{J_{12}^2}{2J_{13}} \quad (1)$$

$$\frac{\omega_{z2}^2 LC - 1}{\omega_{z2} L} = -\frac{\omega_{z2}^2}{\omega_0^2} \cdot \frac{J_{12}^2}{J_{13}} \quad (2)$$

where  $\omega_{z1}$  and  $\omega_{z2}$  correspond to the TZs created by the first and second circuits, respectively;  $\omega_0$  is the resonant frequency of the shunt LC pairs. Since the cross couplings are inductive, i.e.,  $J_{13} > 0$ , the above equations can further yield

$$\begin{cases} \omega_{z1} > 1/\sqrt{LC} = \omega_0 \\ \omega_{z2} < 1/\sqrt{LC} = \omega_0 \end{cases} \quad (3)$$

This indicates that a TZ is created above the passband for the first circuit, whereas it is located below the passband for the second circuit. This is verified in Figures 4 and 5, which depict the EM- and circuit-simulated  $S$ -parameters, demonstrating consistency with the above theoretical results.

## III. Filter Design and Analysis

To obtain a dual-band response, the rectangular SIW cavi-

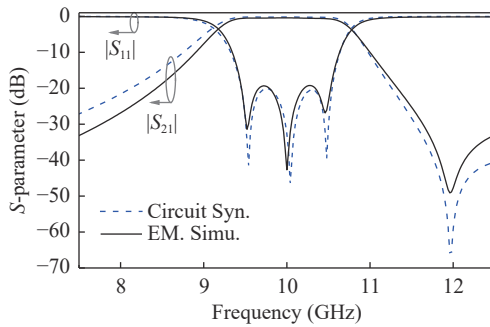


**Figure 4** EM- and circuit-simulated  $S$ -parameters of the meander-line-based SIW triplet. Syn., synthesized; Simu., simulated.

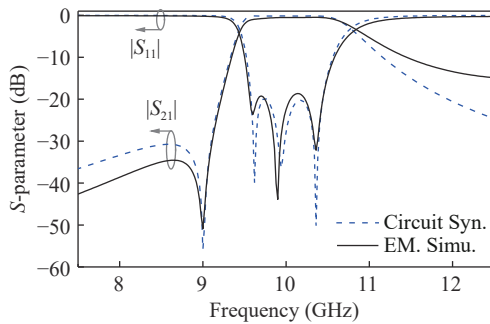


**Figure 5** EM- and circuit-simulated  $S$ -parameters of the CRLH-based SIW triplet.

ties discussed in [21] are used for demonstration, and their  $TE_{101}$  and  $TE_{201}$  modes are utilized to create two passbands operating at 8 GHz and 10 GHz in the X-band. A related discussion on the control of resonant frequencies and external quality factors was provided in [21]. Therefore, in this work, we mainly show how to achieve quasi-elliptic responses on the basis of such rectangular SIW cavities. For this purpose, one fundamental concern is how to incorporate the meander-line and CRLH resonators to constitute proper SIW triplets for the  $TE_{101}$  and  $TE_{201}$  modes, including the numbers and placements of these resonators.

### 1. Place a TZ at the lateral sides of the two passbands

For a dual-band quasi-elliptic filter, a TZ appears at each side of the passband. To illustrate the design procedure, the first step is to allocate a TZ below the first passband and above the second passband. To achieve this goal, a potential strategy is to create a CRLH-based triplet for the  $TE_{101}$  mode and a meander-line-based triplet for the  $TE_{201}$  mode, as presented in Figure 6. To achieve this coupling topology on SIW platforms, Figures 7(a) and (b) show the positions on an SIW cavity that are suitable for coupling the  $TE_{101}$  mode and  $TE_{201}$  mode, respectively. Theoretically, the CRLH resonator can be placed anywhere along the edge of the SIW cavity. Since the  $TE_{201}$  mode has the weakest magnetic field distribution at the center of the cavity edge, the meander-line resonator must be placed on one of the two sides of the SIW edge except for the center. On this basis, Figure 8 depicts six placements for these two resonators between the SIW cavities.

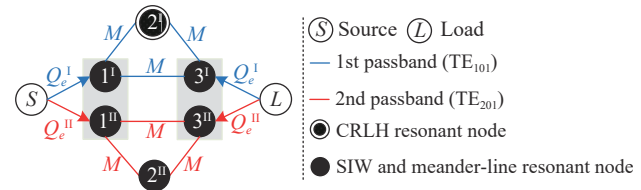


**Figure 6** Coupling topology combining a CRLH-based triplet for the  $TE_{101}$  mode and a meander-line-based triplet for the  $TE_{201}$  mode.

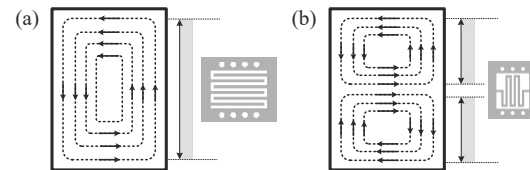


**Figure 7** (a) Positions where the CRLH resonator can be placed to couple the  $TE_{101}$  mode; (b) Positions where the meander-line resonator can be placed to couple the  $TE_{201}$  mode.

1) Cases A and B: The meander-line resonator is placed on the upper side of the SIW cavity, with the CRLH resonator located in two different positions.

2) Cases A' and B': The meander-line resonator is placed on the lower side of the SIW cavity, with the CRLH resonator located in two different positions.

3) Cases C and C': Both the meander-line and CRLH resonators are placed on the upper side of the SIW cavity, but their positions are switched.

An inductive window is introduced to produce cross coupling in all these cases. As shown, they are all able to create a CRLH-based triplet for the  $TE_{101}$  mode and a meander-line-based triplet for the  $TE_{201}$  mode, thus generating a TZ below the first passband and above the second passband. However, thus far, no TZs have been observed between the passbands.

### 2. Allocate TZs between the two passbands

To create a TZ between the passbands, a promising solution is to introduce one more trisection topology. This can be achieved by adding either a meander-line resonator for the  $TE_{101}$  mode or a CRLH resonator for the  $TE_{201}$  mode, thus generating a TZ above the first passband or below the second passband. For validation, Figure 9 shows the planar configuration of the proposed filter utilizing the former means (note that other arrangements may also work), in which a larger meander-line resonator is added to couple the  $TE_{101}$  mode. This design results in a 4-pole response for the first passband, whereas a 3-pole response for the second passband remains.

The coupling schematic topology of the proposed filter is depicted in Figure 10. The first passband is a transverse topology consisting of meander-line-based and CRLH-based triplets, which is able to create a TZ above and below the passband. The second passband is originally produced by the meander-line-based triplet, but the  $TE_{101}$  mode is able to bypass the  $TE_{201}$  mode through the CRLH resonator, as indicated in [23], which is capacitively dominant when the frequency is beyond the first passband.

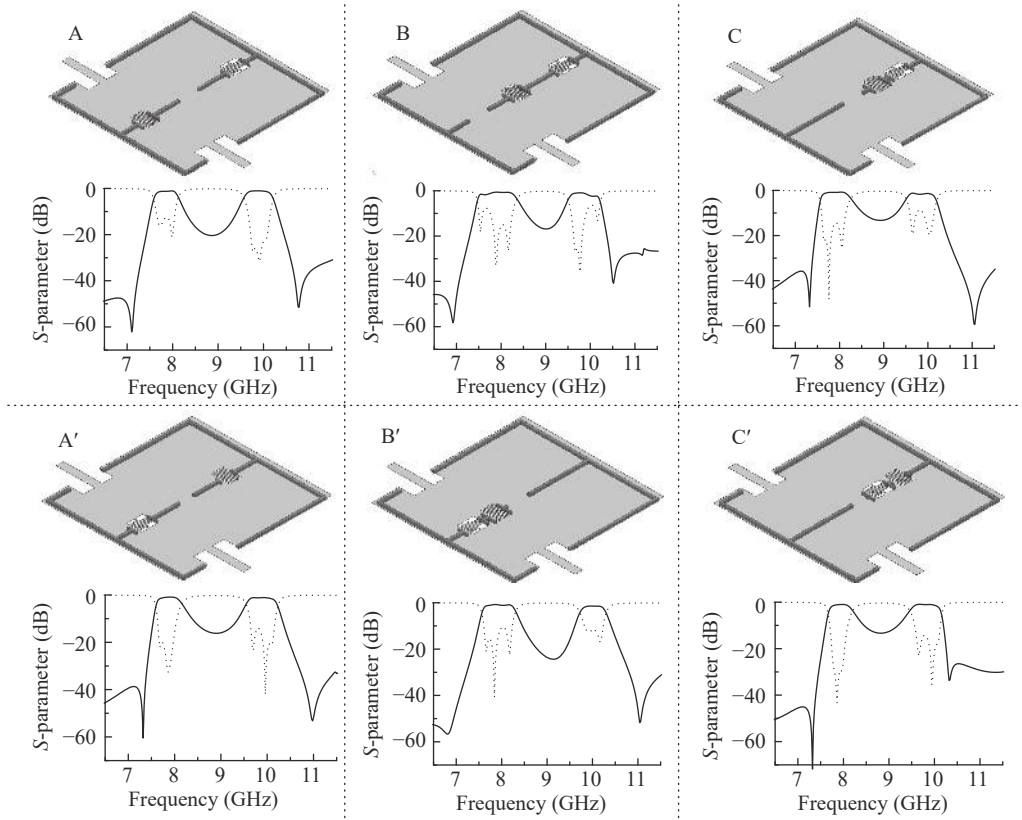


**Figure 8** Six different placements of the CRLH and meander-line resonators.

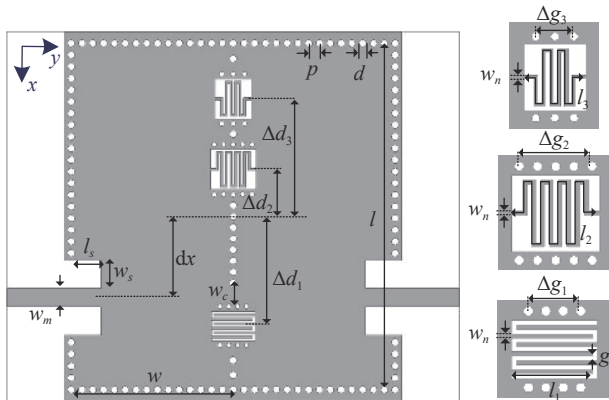


**Figure 9** Layout of the proposed dual-band quasi-elliptic filter and the magnified meander-line and CRLH resonators. (Initial dimensions in mm:  $l = 29.4$ ,  $w = 14.1$ ,  $l + s = 2.6$ ,  $w_s = 2.4$ ,  $w_m = 1.57$ ,  $\Delta d_1 = 9.3$ ,  $\Delta d_2 = 4$ ,  $\Delta d_3 = 10$ ,  $w_c = 2.1$ ,  $dx = 6.9$ ,  $d = 0.6$ ,  $p < 1$ ,  $l_1 = 3.588$ ,  $l_2 = 23.845$ ,  $l_3 = 17.185$ ,  $\Delta g_1 = 2.3$ ,  $\Delta g_2 = 3.3$ ,  $\Delta g_3 = 2$ ,  $w_n = 0.2$ ,  $g = 0.2$ ).

Therefore, an electric bypass coupling can be considered between the source/load and the  $TE_{201}$  mode, which consequently creates another triplet, as shown in **Figure 10**. According to [24], the trisection loops of  $TE_{201}$  modes, which carry magnetic and electric cross coupling, can also produce a TZ above and below the second passband. Therefore, a dual-band quasi-elliptic response can be achieved based on the proposed filter configuration.

### 3. Synthesis and design

For synthesis purposes, the proposed dual-band filter is de-

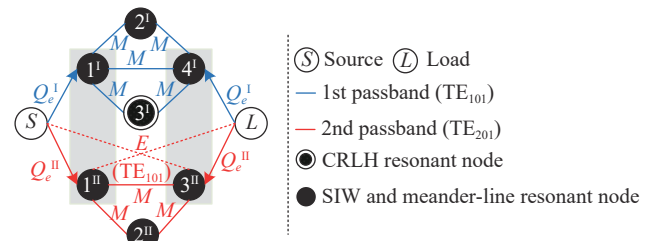


**Figure 10** Coupling topology of the proposed dual-band filter.

signed with a quasi-elliptic response, whose return loss is allotted as 20 dB for both passbands. Two passbands are centered at 8 GHz and 10 GHz ( $f_2/f_1 = 1.25$ ) in the X-band, with corresponding equal-ripple bandwidths of 0.48 GHz ( $\Delta_1 = 6\%$ ) and 0.38 GHz ( $\Delta_2 = 3.8\%$ ), respectively. The finite TZs are placed at 7.52 GHz and 8.64 GHz for the first passband, and at 9.2 GHz and 10.8 GHz for the second passband. The normalized coupling-matrix parameters can be synthesized as

$$Q_e^I = 15.7, k_{12}^I = k_{24}^I = 0.666, k_{13}^I = k_{34}^I = 0.580, k_{14}^I = 0.086$$

$$Q_e^{II} = 22.5, k_{12}^{II} = k_{23}^{II} = 1.017, k_{13}^{II} = 0.066, k_{S3}^{II} = k_{L1}^{II} = -0.0225$$

The coupling coefficients can be tuned by the parameters  $\Delta d_1$ ,  $\Delta d_2$ ,  $\Delta d_3$ ,  $\Delta g_1$ ,  $\Delta g_2$ , and  $\Delta g_3$  in practical filter configurations. **Figure 11** shows the synthesized  $S$ -parameters, which produce a 4-pole response for the first passband and a 3-pole response for the second passband, exhibiting high

selectivity with a TZ located on each side of the two passbands.

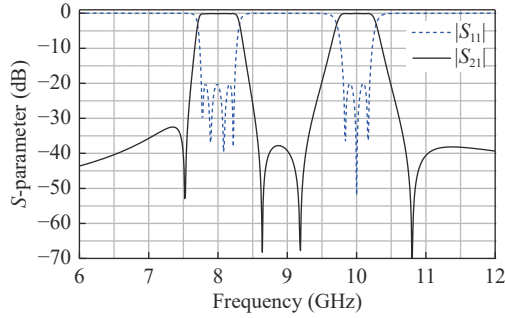


**Figure 11** Synthesized  $S$ -parameters centered at 8 GHz and 10 GHz.

#### IV. Fabrication, Measurement, and Discussion

For validation purposes, the filter was manufactured on a Rogers RT/Duriod 5880 substrate with  $\epsilon_r = 2.2$ , thickness  $h = 508 \mu\text{m}$ , and  $\tan \delta = 0.0009$ . **Figure 12** (a) shows a photograph of the fabricated prototype, which has a compact circuit size of  $31.44 \times 29.4 \text{ mm}^2$  ( $1.14\lambda_g \times 1.06\lambda_g$ ). **Figures 12**(b) and (c) show the electric field distributions at the two center frequencies. The  $\text{TE}_{101}$  mode is coupled to the CRLH and large meander-line resonators, whereas the  $\text{TE}_{201}$  mode transmits through the small meander-line resonator.

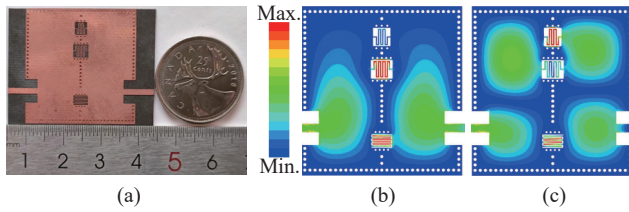


**Figure 12** (a) Photograph of the fabricated filter; (b) Electric field distributions of the 1st passband at 8 GHz and (c) the 2nd passband at 10 GHz. Max., maximum; Min., minimum.

The fabricated circuit was tested with TRL calibration, and its measured and simulated  $S$ -parameters are depicted in **Figure 13**; they are in fairly good agreement. The measured center frequencies are located at 7.97 GHz and 9.95 GHz, respectively, which are slightly lower than the simulated frequencies of 8 GHz and 10 GHz. The measured 3-dB bandwidth of the first passband is 708 MHz, rather

enlarged compared to the simulation of 610 MHz. In contrast, for the second passband, the measured 3-dB bandwidth is 590 MHz, which is almost identical to the simulated 580 MHz bandwidth. Additionally, the measured minimum insertion losses (ILs) for the two passbands are 1.36 dB and 1.15 dB, which are extremely close to the simulated data of 1.24 dB and 1.12 dB, respectively. The in-band return losses are better than 12.1 dB and 18.1 dB. A TZ is generated at each side of the passband, resulting in sharp roll-off for both passbands. Note that the 5<sup>th</sup> TZ at 12 GHz is actually produced by bypass coupling effects, in which the  $\text{TE}_{301}$  mode is weakly bypass coupled with the  $\text{TE}_{201}$  mode. The mechanism of bypass coupling can be found in [23]. Overall, the filter presents good electrical performance with quasi-elliptic responses for both passbands, which show low losses and high selectivity with a TZ created at both sides of each passband.

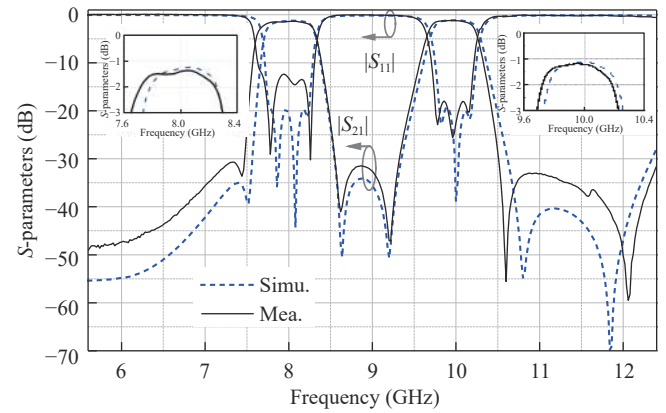


**Figure 13** Simulated and measured  $S$ -parameters of the proposed dual-band filter. Mea., measured.

To the best of the authors' knowledge, only a few dual-band SIW filters with quasi-elliptic responses have been reported [17]–[21]. To reveal advancement of the proposed filter, **Table 1** presents a comparison of our work with these state-of-the-art designs. Compared with the filters in [17]–[20], the filter in this work has the advantage of eliminating negative-coupling structures such as the S-shaped slots in [17], the interdigital formats in [19] and the GCPW lines in [20]. Although a negative-coupling structure is also

**Table 1** Comparison of state-of-the-art filters

| Ref.      | Technology       | Layer  | Response type  | Order | $f_1/f_2$ (GHz) | $k = f_2/f_1$ | 3-dB FBW (%) | ILs (dB)  | No. of TZs | Rejection | Size ( $\lambda_g \times \lambda_g$ ) | Neg.-coupling structures |
|-----------|------------------|--------|----------------|-------|-----------------|---------------|--------------|-----------|------------|-----------|---------------------------------------|--------------------------|
| [17]-III  | SIW              | Single | Quasi-elliptic | 4/4   | 20/21           | 1.05          | 1.75/1.67    | 2.2/1.2   | 5          | >30 dB    | $2.79 \times 1.47$                    | S-shaped slots           |
| [19]-II   | HMSIW            | Single |                | 4/4   | 5.0/8.5         | 1.7           | 6.26/7.75    | 2.02/1.82 | 4          | > 20 dB   | $0.84 \times 1.31$                    | Interdigital formats     |
| [20]-III  | SIW              | Double |                | 4/4   | 12/17           | 1.42          | 6.87/3.26    | 1.16/2.32 | 5          | > 22 dB   | $0.95 \times 1.22$                    | GCPW lines               |
| [21]      | SIW & microstrip | Single |                | 4/4   | 8.05/9.99       | 1.24          | 9.1/6.2      | 1.74/2.21 | 4          | > 40 dB   | $1.13 \times 1.02$                    | N/A                      |
| This work | SIW & microstrip | Single |                | 4/3   | 7.97/9.95       | 1.25          | 8.89/5.93    | 1.36/1.15 | 5          | >30 dB    | $1.14 \times 1.06$                    | N/A                      |

Neg.-coupling, negative-coupling; N/A, not applicable.

not employed in [21], the filter is realized based on the conventional cross-coupled quadruplet. Whereas in this work, the dual-band SIW filter is designed by combining two novel meander-line and CRLH-based triplets, which results in lower insertion losses, and more TZs are created with a lower filter order. In summary, a dual-band quasi-elliptic SIW filter is obtained with all inductive couplings for the first time.

## V. Conclusion

In this work, a novel dual-band quasi-elliptic SIW filter design technique is developed by utilizing meander-line and CRLH-based trisections. Owing to their reversed zero-pole responses, the design procedures, especially the allocation of TZs, are well described in both theory and simulation. The key feature of this technique is its ability to flexibly generate and control TZs with all inductive couplings. With this impressive performance, a dual-band filter centered at 8 GHz and 10 GHz is developed and fabricated for validation. The simulated and measured present indicate outstanding electrical performance of compact size and high selectivity, suggesting that the proposed design technique can be considered an attractive way to implement quasi-elliptic dual-band SIW filters without negative-coupling structures.

## Acknowledgement

This work was supported in part by the Natural Sciences and Engineering Research Council (NSERC) of Canada, and in part by the China Scholarship Council (No. Grant 202006070154).

## References

- [1] P. K. Singh, S. Basu, and Y. H. Wang, "Miniature dual-band filter using quarter wavelength stepped impedance resonators," *IEEE Microwave and Wireless Components Letters*, vol. 18, no. 2, pp. 88–90, 2008.
- [2] S. Cheab, P. W. Wong, and S. Soeung, "Design of multi-band filters using parallel connected topology," *Radioengineering*, vol. 27, no. 1, pp. 186–192, 2018.
- [3] C. M. Tsai, H. M. Lee, and C. C. Tsai, "Planar filter design with fully controllable second passband," *IEEE Transactions on Microwave Theory and Techniques*, vol. 53, no. 11, pp. 3429–3439, 2005.
- [4] Y. L. Wu, L. W. Cui, Z. Zhuang, *et al.*, "A simple planar dual-band bandpass filter with multiple transmission poles and zeros," *IEEE Transactions on Circuits and Systems II: Express Briefs*, vol. 65, no. 1, pp. 56–60, 2018.
- [5] A. Garcia-Lamperoz and M. Salazar-Palma, "Single-band to multi-band frequency transformation for multiband filters," *IEEE Transactions on Microwave Theory and Techniques*, vol. 59, no. 12, pp. 3048–3058, 2011.
- [6] S. B. Zhang and L. Zhu, "Compact split-type dual-band bandpass filter based on  $\lambda/4$  resonators," *IEEE Microwave and Wireless Components Letters*, vol. 23, no. 7, pp. 344–346, 2013.
- [7] X. Tian, H. J. Qian, R. Gómez-García, *et al.*, "Compact K-band split-type dual-band bandpass filter based on stepped-impedance DGS cells," in *Proceedings of the 11th UK-Europe-China Workshop on Millimeter Waves and Terahertz Technologies*, Hangzhou, China, pp. 1–3, 2018.
- [8] S. Sun, "A dual-band bandpass filter using a single dual-mode ring resonator," *IEEE Microwave and Wireless Components Letters*, vol. 21, no. 6, pp. 298–300, 2011.
- [9] W. Jiang, W. Shen, T. X. Wang, *et al.*, "Compact dual-band filter using open/short stub loaded stepped impedance resonators (OSLSIRs/SSLSIRs)," *IEEE Microwave and Wireless Components Letters*, vol. 26, no. 9, pp. 672–674, 2016.
- [10] V. Nocella, L. Pelliccia, C. Tomassoni, *et al.*, "Miniaturized dual-band waveguide filter using TM dielectric-loaded dual-mode cavities," *IEEE Microwave and Wireless Components Letters*, vol. 26, no. 5, pp. 310–312, 2016.
- [11] A. Widaa and M. Höft, "Miniaturized dual-band dual-mode TM-mode dielectric filter in planar configuration," *IEEE Journal of Microwaves*, vol. 2, no. 2, pp. 326–336, 2022.
- [12] A. K. Gorur and C. Karpuz, "A novel perturbation arrangement for dual-mode resonators and its dual-band bandpass filter applications," in *Proceedings of the 41st European Microwave Conference*, Manchester, UK, pp. 468–471, 2011.
- [13] W. Shen, W. Y. Yin, and X. W. Sun, "Miniaturized dual-band substrate integrated waveguide filter with controllable bandwidths," *IEEE Microwave and Wireless Components Letters*, vol. 21, no. 8, pp. 418–420, 2011.
- [14] M. K. Li, C. Chen, and W. D. Chen, "Miniaturized dual-band filter using dual-capacitively loaded SIW cavities," *IEEE Microwave and Wireless Components Letters*, vol. 27, no. 4, pp. 344–346, 2017.
- [15] A. R. Azad and A. Mohan, "Substrate integrated waveguide dual-band and wide-stopband bandpass filters," *IEEE Microwave and Wireless Components Letters*, vol. 28, no. 8, pp. 660–662, 2018.
- [16] A. R. Azad and A. Mohan, "Substrate integrated waveguide dual-band bandpass filter," in *Proceedings of the 8th Uttar Pradesh Section International Conference on Electrical, Electronics and Computer Engineering*, Dehradun, India, pp. 1–6, 2021.
- [17] X. P. Chen, K. Wu, and Z. L. Li, "Dual-band and triple-band substrate integrated waveguide filters with Chebyshev and quasi-elliptic responses," *IEEE Transactions on Microwave Theory and Techniques*, vol. 55, no. 12, pp. 2569–2578, 2007.
- [18] K. Zhou, C. X. Zhou, and W. Wu, "Resonance characteristics of substrate-integrated rectangular cavity and their applications to dual-band and wide-stopband bandpass filters design," *IEEE Transactions on Microwave Theory and Techniques*, vol. 65, no. 5, pp. 1511–1524, 2017.
- [19] K. Zhou, C. X. Zhou, and W. Wu, "Dual-mode characteristics of half-mode SIW rectangular cavity and applications to dual-band filters with widely separated passbands," *IEEE Transactions on Microwave Theory and Techniques*, vol. 66, no. 11, pp. 4820–4829, 2018.
- [20] K. Zhou, C. X. Zhou, and W. Wu, "Substrate-integrated waveguide dual-mode dual-band bandpass filters with widely controllable bandwidth ratios," *IEEE Transactions on Microwave Theory and Techniques*, vol. 65, no. 10, pp. 3801–3812, 2017.
- [21] Y. L. Zhu and Y. D. Dong, "A compact dual-band quasi-elliptic filter based on hybrid SIW and microstrip technologies," *IEEE Transactions on Circuits and Systems II: Express Briefs*, vol. 69, no. 3, pp. 719–723, 2022.
- [22] Y. L. Zhu, Y. D. Dong, J. Bornemann, *et al.*, "SIW triplets including meander-line and CRLH resonators and their applications to quasi-elliptic filters," *IEEE Transactions on Microwave Theory and Techniques*, vol. 71, no. 5, pp. 2193–2206, 2023.
- [23] S. Amari and U. Rosenberg, "Characteristics of cross (bypass) coupling through higher/lower order modes and their applications in elliptic filter design," *IEEE Transactions on Microwave Theory and Techniques*, vol. 53, no. 10, pp. 3135–3141, 2005.
- [24] S. Sirci, J. D. Martínez, J. Vague, *et al.*, "Substrate integrated waveguide diplexer based on circular triplet combline filters," *IEEE Microwave and Wireless Components Letters*, vol. 25, no. 7, pp. 430–432, 2015.



**Yilong Zhu** received the B.E. degree from University of Electronic Science and Technology of China (UESTC), Chengdu, China, in 2015, the M.S. degree from Beihang University, Beijing, China, in 2018, and the Ph.D. degree in electromagnetic field and microwave techniques from UESTC, Chengdu, China, in 2023. He was a Visiting Ph.D. Student with the Department of Electrical and Computer Engineering, University of Victoria, Victoria, BC, Canada, During March 2021 to December 2022. He has been an Assistant Research Fellow with the Aerospace Information Research Institute, Chinese Academy of Sciences, Beijing, China, since 2023. His research interests include remote sensing, signal processing, synthesis design of planar microwave and mm-wave filters/diplexers. (Email: [yilongzhu@ieee.org](mailto:yilongzhu@ieee.org))



**Yuandan Dong** received the B.S. and M.S. degrees from Southeast University, Nanjing, China, in 2006 and 2008, respectively, and the Ph.D. degree from University of California at Los Angeles, Los Angeles, CA, USA, in 2012. Since 2017, He has been a Full Professor with the University of Electronic Science and Technology of China, Chengdu, China. His research interests include the characterization and development of RF and microwave components, antennas, RF front-end modules, circuits, acoustic-wave filters, and metamaterials.

Dr. Dong has authored or coauthored more than 290 journal articles and conference papers, which received more than 6900 citations. He has been listed as an Elsevier highly cited researcher. He holds more than 100 patents including seven international patents. He has been a TPC member for several international conferences. He has served as an Associate Editor with outstanding service award for the IEEE Transactions on Antennas and Propagation since 2021, and he has served as a Guest Editor for IEEE Open Journal of Antennas and Propagation. He is also serving as a Reviewer for multiple IEEE and IET journals, including the IEEE Transactions on Microwave Theory and Techniques and the IEEE Transactions on Antennas and Propagation. (Email: [ydong@uestc.edu.cn](mailto:ydong@uestc.edu.cn))



**Lin Gu** received the B.S. degree from Nanchang Hangkong University, Nanchang, China, in 2020, and the M.S. degree from University of Electronic Science and Technology of China, Chengdu, China, in 2023, where she is currently pursuing the Ph.D. degree in electromagnetic field and microwave techniques. Her research interests include planar hybrid filter, IPD filter, and acoustic-wave filters for wireless communication.

(Email: [825641270@qq.com](mailto:825641270@qq.com))



**Deisy Formiga Mamedes** received the B.S. and the MS. degrees in electrical engineering, from the Federal Institute of Paraiba, Paraiba, Brazil, in 2016 and 2018, respectively. She is currently pursuing the Ph.D. degree in electrical engineering at the University of Victoria, Victoria, BC, Canada.

She worked as an instructor during 2017 to 2018 at the Federal Institute of Rio Grande do Norte, XXXX, Brazil, and during 2018 to 2019 at the Senai College of Paraiba, Paraiba, Brazil. During 2022 to 2023, she was a Sessional Instructor with the University of Victoria, Victoria, Canada. She worked as RFIC designer and lab measurements co-op at Skyworks Solutions, XXXX, Canada, in 2023. In 2024, she joined the Herzberg Astronomy and Astrophysics (HAA), National Research Council Canada (NRC), XXXX, Canada. She has authored/coauthored over 40 technical papers. Her research interests include microwave and millimeter-wave components, modeling of integrated circuits, frequency-selective surfaces, antennas and low-noise amplifiers. (Email: [mamedes@ieee.org](mailto:mamedes@ieee.org))



**Jens Bornemann** received the Dipl.-Ing. and Dr.-Ing. degrees in electrical engineering from the University of Bremen, Bremen, Germany, in 1980 and 1984, respectively.

From 1984 to 1985, he worked as an engineering consultant. In 1985, he joined the University of Bremen, Bremen, Germany, as an Assistant Professor. During April 1988 to December 2023, he has been with the Department of Electrical and Computer Engineering, University of Victoria, Victoria, BC, Canada, where he became a Professor in 1992. Since January 2024, he has been a Professor Emeritus and Adjunct Professor with the same department. He has coauthored *Waveguide Components for Antenna Feed Systems—Theory and Design* (Artech House, 1993) and has authored/coauthored more than 400 technical papers. His research activities include RF/wireless/microwave/millimeter-wave components, systems and antenna design, and field-theory-based modeling of integrated circuits, feed networks and antennas.

Dr. Bornemann served as an Associate Editor for the IEEE Transactions on Microwave Theory and Techniques in the area of Microwave Modeling and CAD during 1999 to 2002, and International Journal of Electronics and Communications during 2006 to 2008. He was a Registered Professional Engineer in the Province of British Columbia, Canada. He is a Life Fellow of IEEE, a Fellow of the Canadian Academy of Engineering (CAE), a Fellow of the Engineering Institute of Canada and serves on the editorial advisory board of the International. (Email: [j.bornemann@ieee.org](mailto:j.bornemann@ieee.org))